molecular pharmaceutics

Article

pubs.acs.org/molecularpharmaceutics

Comparison of Conjugation Strategies of Cross-Bridged Macrocyclic Chelators with Cetuximab for Copper-64 Radiolabeling and PET Imaging of EGFR in Colorectal Tumor-Bearing Mice

Dexing Zeng,[†,‡] Yunjun Guo,[‡,§,∥] Alexander G. White,[†] Zhengxin Cai,[†] Jalpa Modi,[†] Riccardo Ferdani,[§] and Carolyn J. Anderson*[,†,⊥,#]

[†]Departments of Radiology, [⊥]Pharmacology and Chemical Biology, and [#]Bioengineering, University of Pittsburgh, Pittsburgh, Pennsylvania, United States

[§]Mallinckrodt Institute of Radiology and [∥]Department of Chemistry, Washington University, St. Louis, Missouri, United States

Supporting Information

ABSTRACT: Epidermal growth-factor receptor (EGFR) is overexpressed in a wide variety of solid tumors and has served as a well-characterized target for cancer imaging and therapy. Cetuximab was the first mAb targeting EGFR approved by the FDA for the treatment of metastatic colorectal and head and neck cancers. Previous studies showed that ^{64}Cu ($T_{1/2}$ = 12.7 h; β^+ (17.4%)) labeled DOTA−cetuximab showed promise for PET imaging of EGFR-positive tumors; however the *in vivo* stability of this compound has been questioned. In this study, two recently developed cross-bridged macrocyclic chelators (CB-TE1A1P and CB-TE1K1P) were conjugated to cetuximab using standard NHS coupling procedures and/or strain-promoted azide−alkyne cycloaddition (SPAAC) methodologies. The radiolabeling and *in vitro*/*vivo* evaluation of the resulting cetuximab conjugates were compared. Improved Cu-64 labeling efficiency and high specific activity (684 kBq/μg, decay corrected to the end of bombardment) were obtained with the CB-TE1K1P-PEG$_4$-click-cetuximab conjugate. Saturation binding assays indicated that the prepared cetuximab conjugates had comparable affinity (1.32−2.00 nM) in the HCT116 human colorectal tumor cell membranes. In the subsequent *in vivo* evaluation, ^{64}Cu-CB-TE1K1P-PEG$_4$-click-cetuximab demonstrated more rapid renal clearance with a higher tumor/nontumor ratio than other ^{64}Cu-labeled cetuximab conjugates, and it shows the greatest promise for imaging and therapy of EGFR-positive tumors.

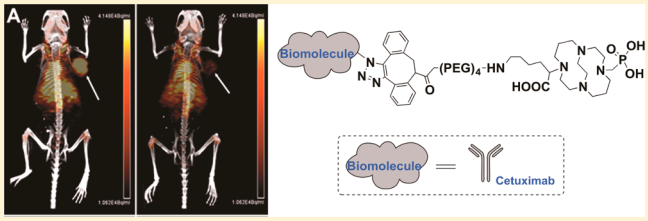

KEYWORDS: *copper-64, cetuximab, epidermal growth-factor receptor, cross-bridged chelator, metal-free click chemistry, PET imaging*

INTRODUCTION

Epidermal growth-factor receptor (EGFR) is overexpressed in a wide variety of solid tumors and has served as a well-characterized target for cancer imaging and therapy,[1] and it is associated with many human malignancies including head and neck, colorectal, non-small cell lung, and breast cancers, among others.[2] Overexpression of EGFR in tumors is correlated with aggressive disease, poor prognosis, poor response, and resistance to cytotoxic therapy in some tumor types.[3] Cetuximab (C225, Erbitux) is a recombinant human/mouse chimeric immunoglobulin G1 (IgG1) monoclonal antibody (mAb) that binds specifically to the extracellular domain of EGFR with high affinity. It was approved by the US Food and Drug Administration in 2004 for the treatment of patients with EGFR-expressing, metastatic colorectal cancer. Cetuximab blocks the activation of EGFR by preventing ligand-mediated tyrosine kinase phosphorylation and downstream signal transduction, which induces the internalization and possible degradation of EGFR.[4] Several clinical trials have shown that cetuximab, either administered alone or combined with the standard first or second line chemotherapy, improved treatment efficacy for metastatic colorectal cancer without a significant increase in toxicity.[5−7]

There has been significant interest in radiolabeled cetuximab since the unlabeled drug was FDA-approved for the treatment of colorectal cancer. Cetuximab has been radiolabeled with ^{99m}Tc and ^{111}In for SPECT imaging[8,9] and ^{64}Cu, ^{86}Y, and ^{89}Zr for PET imaging.[10−12] Copper-64 ($T_{1/2}$ = 12.7 h) is particularly promising because of its suitable half-life and unique decay characteristics: β^+ (656 keV, 17.4%) and β^- (573 keV, 38.5%), and the beta-decay makes this radionuclide attractive for therapy.[13−16] Radiolabeling at 37 °C or below is critical to maintain the biological integrity of antibodies, therefore DOTA has been the most commonly used chelator for ^{64}Cu radiolabeling of cetuximab and other antibodies. However, the *in vivo* behavior of the ^{64}Cu-DOTA complex is less than

Special Issue: Positron Emission Tomography: State of the Art

Received: January 3, 2014
Revised: March 13, 2014
Accepted: April 10, 2014
Published: April 10, 2014

optimal due to dissociation of ^{64}Cu from the DOTA complex, and this might lead to relatively poor tumor to nontumor ratios.[10,17,18] Cross-bridged macrocyclic chelators (such as CB-TE2A, CB-TE1A1P, and CB-TE1K1P, Figure 1) have shown

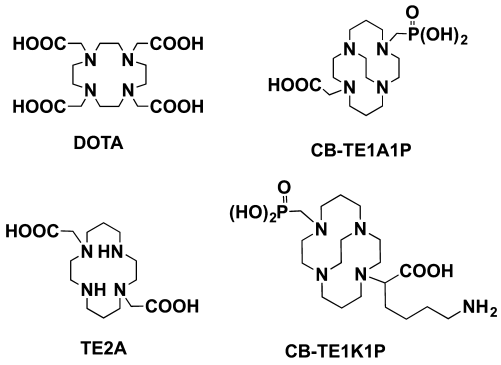

Figure 1. Structures of DOTA, CB-TE2A, CB-TE1A1P, and CB-TE1K1P.

impressive kinetic inertness for Cu complexes.[19−22] The monocarboxylate monophosphonate chelator CB-TE1A1P can be labeled with ^{64}Cu at room temperature with comparable *in vivo* stability to CB-TE2A,[21] and its peptide conjugate ^{64}Cu-CB-TE1A1P-Y3-TATE demonstrated improved tumor targeting and biodistribution compared to ^{64}Cu-CB-TE2A-Y3-TATE conjugate in a pancreatic tumor bearing rat model.[23] The newly developed CB-TE1K1P chelator, containing one methanephosphonate and one carboxylate pendant group, has advantages due to the maintenance of the carboxylate group postconjugation to biomolecules, and this chelator may be an improved bifunctional chelator for the labeling of copper radionuclides to monoclonal antibodies, such as cetuximab.[22]

Herein, the two cross-bridged chelators CB-TE1A1P and CB-TE1K1P were conjugated to cetuximab via conventional NHS (*N*-hydroxysuccinimide) ester conjugation and/or strain-promoted azide−alkyne cycloaddition (SPAAC) strategies, and the resulting conjugates were evaluated in nude mice bearing HCT116 human colorectal tumors. Besides comparison of the direct conjugation of the NHS ester of CB-TE1A1P to cetuximab using standard coupling techniques to the SPAAC conjugations of CB-TE1A1P and CB-TE1K1P to cetuximab, we address whether the SPAAC approach will achieve greater ease of radiolabeling in higher specific activity (SA) compared to the conventional NHS-ester conjugation strategies. We also investigated whether conjugating the CB-TE1K1P chelator to cetuximab will result in improved targeting and biodistribution compared to CB-TE1A1P that utilizes one of the carboxylates for conjugation.

MATERIALS AND METHODS

Unless specified, all chemicals were purchased from Sigma-Aldrich Chemical Co. (St. Louis, MO). Copper-64 was purchased from Washington University (St. Louis, MO) and the University of Wisconsin (Madison, WI). DBCO-PEG$_4$-NHS ester and DBCO-amine were purchased from Click Chemistry Tools (Scottsdale, AZ). CB-TE1K1P-PEG$_4$-DBCO, CB-TE1A1P-DBCO, and 3-azidopropionic acid succinimidyl ester were synthesized as previously reported.[22] Centricon 100 concentrators were purchased from Amicon (Beverly, MA). Zeba spin desalting columns were from Thermo Scientific (Rockford, IL). Cetuximab was obtained from ImClone Systems Incorporated (New York, NY). Size-exclusion HPLC was performed on a Superose 12 HR 10/300 column (Amersham Biosciences, Uppsala, Sweden), attached to a Waters 600E (Milford, MA) chromatography system with a Waters 991 photodiode array detector and an Ortec model 661 (EG&G Instruments, Oak Ridge, TN) radioactivity detector. The mobile phase was 20 mM HEPES, 150 mM NaCl, pH 7.3 eluted at a flow rate of 0.5 mL/min. Millenium 32 software (Waters, Milford, MA) was used in analyzing the HPLC chromatograms. MultiScreen 96-well microtiter plates for receptor binding assays were counted on a 1450 Microbeta Trilux Liquid Scintillation and Luminescence counter (PerkinElmer Life Sciences).

Conjugation of CB-TE1A1P to Cetuximab and Radiolabeling with ^{64}Cu. The NHS-ester aided conjugation of CB-TE1A1P to cetuximab is shown in Scheme 1. CB-TE1A1P (5.8

Scheme 1. Synthesis of CB-TE1A1P−Cetuximab

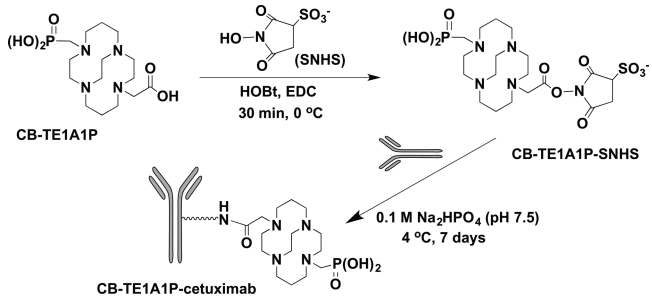

mg, 15 μmol) was mixed with sulfo-*N*-hydroxysuccinimide (SNHS,1.7 mg, 15 μmol) and HOBT (2.0 mg, 15 μmol) in 1 mL of DMF. The coupling reagent 1-ethyl-3-(3-(dimethylamino)propyl)carbodiimide (EDC, 2.9 mg, 15 μmol) was added to the mixture to start the reaction. After 30 min of stirring on ice, the reaction mixture was evaporated to dryness. The concentrated cetuximab (20 mg/mL) was mixed with activated CB-TE1A1P in a 100:1 molar ratio (CB-TE1A1P:cetuximab), followed by incubation at 4 °C for 7 days with end-over-end rotation. The conjugate was then transferred to a Centricon 100, washed twice with 0.1 M ammonium acetate (pH 8.0), and concentrated before being loaded onto a desalting column. Unreacted small molecules were removed by passing the reaction mixture 2−3 times through desalting columns. Purity and concentration of the conjugated cetuximab were determined by size-exclusion HPLC. The number of chelators per antibody was determined by titration of CB-TE1A1P−cetuximab with [^{nat}Cu]copper acetate/^{64}Cu-acetate using a published method.[24] For radiolabeling, ^{64}CuCl$_2$ was added to CB-TE1A1P−cetuximab in 0.1 M ammonium acetate (pH 8.0), followed by incubation at 40 °C for 2 h. The radiochemical purity of ^{64}Cu-CB-TE1A1P−cetuximab was determined by size-exclusion HPLC, and desalting columns were used for purification if necessary.

Click Chemistry and Radiochemistry of CB-TE1K1P-PEG$_4$-DBCO and CB-TE1A1P-DBCO. The synthesis of CB-TE1A1P and CB-TE1K1P attached cetuximab conjugates via SPAAC is shown in Scheme 2. Cetuximab (2.0 mg/mL, 20.0 mL) was functionalized with azide groups by mixing with 3-azidopropionic acid succinimidyl ester (1.27 mg in 1.0 mL of DMF) in Na$_2$HPO$_4$ buffer (0.1 M, pH = 8.2, 5.0 mL) overnight at 4 °C, and then the mixture was transferred to a Centricon 100 and washed with 0.1 M ammonium acetate (pH 8.0) 5−6

dx.doi.org/10.1021/mp500004m | *Mol. Pharmaceutics* 2014, 11, 3980−3987

Scheme 2. Synthesis of CB-TE1A1P-click-cetuximab and CB-TE1K1P-PEG$_4$-click-cetuximab

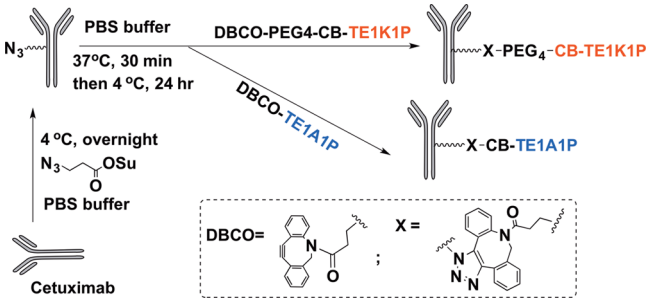

times. The purified azide−cetuximab (2.0 mg/mL) was then mixed with 100-fold excess CB-TE1K1P-PEG$_4$-DBCO or CB-TE1A1P-DBCO and incubated for 30 min at 37 °C, followed by incubation overnight at 4 °C with end-over-end rotation. The reaction was transferred to a Centricon 100, washed with 0.1 M ammonium acetate (pH 8.0) 3−4 times, and loaded onto a desalting column to remove the unreacted DBCO-chelator. The purity and concentration of the chelator−cetuximab conjugates were determined by size-exclusion HPLC. Titration of the chelator−cetuximab with [^{nat}Cu]copper/^{64}Cu-acetate was conducted to measure the number of chelators per antibody. Copper-64-labeled click-chelator cetuximab conjugates were prepared by adding $^{64}CuCl_2$ to the conjugate in 0.1 M ammonium acetate (pH 8.0), followed by incubation at 37 °C for 30 min for CB-TE1K1P-PEG$_4$-DBCO-conjugated antibody and 40 °C for 60 min for CB-TE1A1P-DBCO−cetuximab. Purity of the ^{64}Cu-click-chelator cetuximab conjugates was confirmed by size-exclusion HPLC.

Cell Line and Animal Model. HCT116 cells were provided by Dr. Bert Vogelstein (Johns Hopkins University) and were cultured in DMEM medium supplemented with 10% FBS and 0.1% gentamicin in a 37 °C humidified 95% air, 5% CO_2 incubator. All animal experiments were conducted in compliance the Institutional Care and Use Committees (IACUC) at Washington University and the University of Pittsburgh. Female athymic nude mice (5−6 weeks) were purchased from the NCI (Frederick, MD). For biodistribution studies and small animal PET/CT imaging, 4×10^6 HCT116 cells in 100 μL of 0.9% saline were implanted subcutaneously into the dorsal flank of each animal, and the mice were subjected to biodistribution and/or PET/CT imaging when the tumor volume reached 100 to 200 mm^3 (2−3 weeks).

***In Vitro* Binding Affinity.** The affinity of ^{64}Cu-labeled cetuximab conjugates for EGFR was determined by a saturation binding assay based on previously published methods.[25] HCT116 cell membrane preparations were diluted in binding buffer [0.1% bovine serum albumin, 50 mM Tris-HCl (pH 7.4), 5.0 mmol/L $MgCl_2$, 0.5 μg/mL aprotinin, 200 μg/mL bacitracin, 10 μg/mL leupeptin, and 10 μg/mL pepstatin A], and 15 μg of membrane was added to each well of a 96-well filtration plate (Multiscreen Durapore; Millipore; Billerica, MA). Membranes were incubated with increasing concentrations of ^{64}Cu-labeled cetuximab conjugates for 2 h at room temperature. Nonspecific binding was determined by saturating receptors with excess cetuximab. When equilibrium was reached, unbound radioactivity was filtered off and the membranes were washed twice with 200 μL of binding buffer. Bound radioactivity was measured with a liquid scintillation and luminescence plate reader (1450 Microbeta; PerkinElmer; Waltham, MA). Total binding sites (B_{max}) and binding affinity (K_d) were determined by a nonlinear regression fit of bound peptides per mg of protein versus concentration of radioligand using GraphPad Prism v 5.0 (San Diego, CA).

***In Vivo* Biodistribution.** The biodistribution studies were carried out as previously described.[10] Copper-64-labeled cetuximab (~0.74 MBq, 1.0−6.0 μg in 150 μL) was injected via tail vein into HCT116 tumor-bearing mice (7−9 weeks). At 24 and 48 h after injection, mice were sacrificed and selected organs were removed, weighed, and counted on a γ counter (Beckman 8000; Irvine, CA). A blocking study was also conducted to examine the specificity of *in vivo* uptake. Cetuximab (1 mg) was preinjected 24 h prior to ^{64}Cu-labeled cetuximab conjugates into HCT116 tumor-bearing mice via tail vein. Tissue uptake was measured at 24 h after injection.

Small Animal PET/CT Imaging. HCT116 tumor-bearing female nude mice (7−9 weeks) were injected with ^{64}Cu-labeled cetuximab (~3.7 MBq, 6−30 μg in 150 μL). At 24 and 48 h after injection, the mice were anesthetized with 1−2% isoflurane and imaged. A blocking study was conducted in two tumor-bearing mice as described above. The blocking mice were each paired with nonblocked mice and imaged at the same time points. Tumor standard uptake values (SUV) were generated by measuring regions of interest from PET/CT images and calculated with the formula SUV = [nCi/mL] × [animal weight]/injected dose [nCi].[20]

Statistical Analysis. The data are expressed as mean ± SD. When more than two data sets were compared, two-way ANOVA analysis with Bonferroni post-tests was used. P values <0.05 were considered statistically significant.

RESULTS

Conjugation of CB-TE1A1P to Cetuximab and Radiolabeling with ^{64}Cu. We initially performed conjugation of CB-TE1A1P and cetuximab via the conventional NHS-aided reaction to form an amide bond between the carboxylic acid of CB-TE1A1P and the primary amines of cetuximab. The SA of ^{64}Cu-CB-TE1A1P−cetuximab made by the NHS-aided reaction ranged from 60 to 129 MBq/mg (8700−19,000 MBq/μmol) corrected to end-of-bombardment (EOB) for copper-64. The CB-TE1A1P:cetuximab ratio was 1.5 for CB-TE1A1P−cetuximab synthesized via NHS-aided reactions, compared to 5 chelators/mAb for previously reported DOTA−cetuximab.[10] The low ratio of the chelator to antibody is likely responsible for the lower SA of ^{64}Cu-CB-TE1A1P−cetuximab compared to the DOTA and CB-TE1K1P-PEG$_4$-DBCO conjugates.

Conjugation of CB-TE1K1P-PEG$_4$-DBCO to Cetuximab and Radiolabeling with ^{64}Cu. In the conjugation of CB-TE1K1P-PEG$_4$-DBCO to azide−cetuximab, a 100-fold of excess CB-TE1K1P-PEG$_4$-DBCO was used to ensure that all the azides in cetuximab were conjugated with chelator. The resulting CB-TE1K1P-PEG$_4$-click-cetuximab conjugate was purified by Centricon 100 and a desalting column, and then radiolabeled with ^{64}Cu at a yield >95% after incubation for 30 min at 37 °C. The SA of the ^{64}Cu-CB-TE1K1P-PEG$_4$-click-cetuximab ranged from 548 to 684 MBq/mg (80,000 to 100,000 MBq/μmol). The conjugation ratio averaged 9 chelators per cetuximab, approximately 6 times greater than for CB-TE1A1P−cetuximab. Even at this high chelator:mAb ratio, the binding affinity of the click chemistry conjugate was not compromised.

Conjugation of CB-TE1A1P-DBCO to Cetuximab and Radiolabeling with ^{64}Cu. CB-TE1A1P-DBCO (100 equiv)

Table 1. EGFR Binding Properties of ^{64}Cu-CB-TE1K1P-PEG$_4$-click-cetuximab, ^{64}Cu-CB-TE1A1P-click-cetuximab, ^{64}Cu-CB-TE1A1P−cetuximab, and ^{64}Cu-DOTA−cetuximab[a]

chelator	chelators per antibody	pH	reaction T (°C)	reaction time (min)	SA (kBq/μg)	K_d (nM)	B_{max} (fmol/mg)
click-CB-TE1K1P	9	8.2	37	30	684	1.43 ± 0.41	951 ± 91
click-CB-TE1A1P	9	8.2	40	60	321	1.32 ± 0.42	800 ± 64
nonclick CB-TE1A1P	1.5	8.2	40	120	129	2.00 ± 0.60	1100 ± 120
DOTA	5	7.4	37	30	296	1.89 ± 0.66	848 ± 94

[a] B_{max}: total number of binding sites.

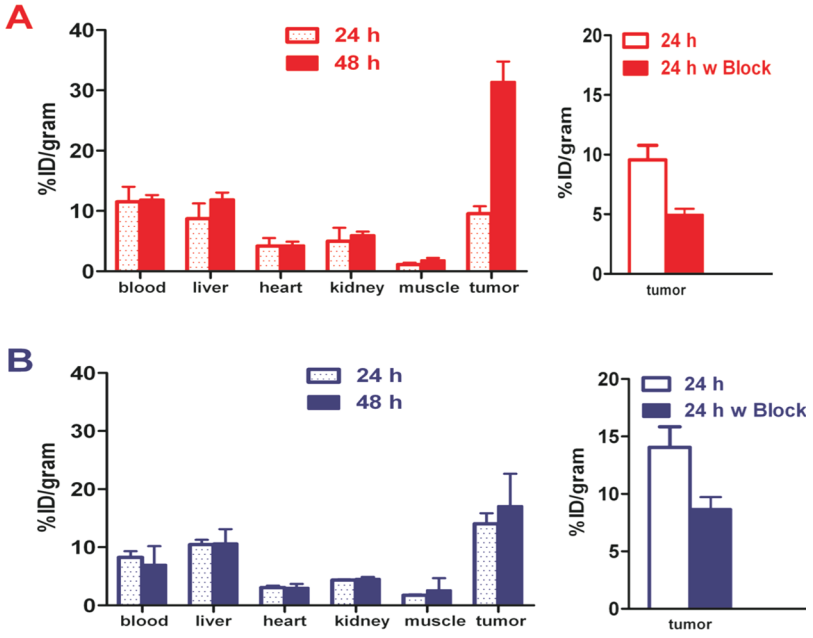

Figure 2. Biodistribution of ^{64}Cu-CB-TE1K1P-PEG$_4$-click-cetuximab (A) and ^{64}Cu-CB-TE1A1P−cetuximab (B) was conducted in HCT116 tumor-bearing female nude mice. Separate blocking studies were performed to confirm the specificity of probes for EGFR, respectively. Data are presented as percent injected dose per gram (n = 3−5 for each data point; bars ± SD).

was used to react with the azido−cetuximab. The resulting CB-TE1A1P-click-cetuximab conjugate (9 chelators per mAb) was purified by Centricon 100 and a desalting column, and the radiolabeling yield was >90% after incubation for 60 min at 40 °C. The SA of the ^{64}Cu-CB-TE1A1P-click-cetuximab ranged from 206 to 321 MBq/mg (30,000 to 47,000 MBq/μmol). Aggregation was observed after radiolabeling of CB-TE1A1P-click-cetuximab, as evidenced by size-exclusion HPLC.

***In Vitro* Binding Affinity.** The dissociation constant (K_d) values of ^{64}Cu-CB-TE1A1P−cetuximab, ^{64}Cu-CB-TE1A1P-click-cetuximab, ^{64}Cu-CB-TE1K1P-PEG$_4$-click-cetuximab, and ^{64}Cu-DOTA−cetuximab for EGFR were 2.00 ± 0.60 nM, 1.32 ± 0.42 nM, 1.43 ± 0.41 nM, and 1.89 ± 0.66 nM respectively (Table 1), and these values are similar to the previous reported K_d of DOTA-cetuximab.[26]

***In Vivo* Biodistribution.** Due to the aggregation of ^{64}Cu-CB-TE1A1P-click-cetuximab, only ^{64}Cu-CB-TE1A1P−cetuximab and ^{64}Cu-CB-TE1K1P-PEG$_4$-click-cetuximab were evaluated in biodistribution studies. The biodistributions were conducted in female nude mice bearing HCT116 tumors. As shown in Figure 2, both agents demonstrated little to no blood clearance from 24 to 48 h (8.2 ± 1.1% ID/g at 24 h to 8.3 ± 1.1% ID/g at 48 h for ^{64}Cu-CB-TE1A1P−cetuximab, and 11.5 ± 2.5% ID/g at 24 h to 11.9 ± 0.8% ID/g at 48 h for ^{64}Cu-CB-TE1K1P-PEG$_4$-click-cetuximab). The radioactivity in the liver also showed either no clearance or slightly increased uptake, from 10.4 ± 0.8% ID/g at 24 h to 9.5 ± 0.2% ID/g at 48 h for ^{64}Cu-CB-TE1A1P−cetuximab, and 8.7 ± 2.5% ID/g at 24 h to 13.1 ± 2.6% ID/g at 48 h for ^{64}Cu-CB-TE1K1P-PEG$_4$-click-cetuximab. For both agents, the amount of activity localized in the kidney, heart, and muscle were lower than the liver, and did not show significant clearance from 24 to 48 h.

^{64}Cu-CB-TE1A1P−cetuximab and ^{64}Cu-CB-TE1K1P-PEG$_4$-click-cetuximab showed increasing tumor uptake from 24 to 48 h. The tumor uptake of ^{64}Cu-CB-TE1K1P-PEG$_4$-click-cetuximab at 48 h postinjection (36.5 ± 1.9% ID/g) was three times higher than the tumor uptake at 24 h postinjection (9.6 ± 1.2% ID/g). The tumor uptake of ^{64}Cu-CB-TE1A1P−cetuximab also increased 1.5 times from 24 h (14.1 ± 1.8% ID/g) to 48 h (20.2 ± 6.1% ID/g) after the administration of agents. The % injected dose in the tumor was greatest at 48 h postinjection for both ^{64}Cu-CB-TE1K1P-PEG$_4$-click-cetuximab and ^{64}Cu-CB-TE1A1P−cetuximab (p's < 0.05 compared to values at other time points). The specificity of ^{64}Cu-CB-TE1A1P−cetuximab and ^{64}Cu-CB-TE1K1P-PEG$_4$-click-cetuximab for EGFR was confirmed by separate blocking studies performed at 24 h postinjection. Preinjecting 1.0 mg of cold cetuximab reduced tumor uptake of ^{64}Cu-CB-TE1A1P−cetuximab from 14.1 ± 1.78% ID/g to 8.68 ± 1.03% ID/g (p < 0.05), and that of ^{64}Cu-CB-TE1K1P-PEG$_4$-click-cetuximab from 9.5 ± 1.2% ID/g to 4.9 ± 0.5% ID/g (p < 0.05).

The comparison of tumor:nontumor ratios at 48 h postinjection among ^{64}Cu-CB-TE1K1P-PEG$_4$-click-cetuximab, ^{64}Cu-CB-TE1A1P−cetuximab, and ^{64}Cu-DOTA−cetuximab[27]

is shown in Figure 3. The tumor:muscle and tumor:liver ratios of ^{64}Cu-CB-TE1K1P-PEG$_4$-click-cetuximab were significantly higher than those of ^{64}Cu-DOTA−cetuximab ($p < 0.001$, $p < 0.01$ respectively), whereas the tumor:blood showed a higher trend but the differences were not significant ($p = 0.09$). On the other hand, compared to ^{64}Cu-DOTA−cetuximab, ^{64}Cu-CB-TE1A1P−cetuximab showed comparable tumor:blood and tumor:liver ratios, but significantly lower tumor:muscle and tumor:kidney ratios ($p < 0.05$ for both), which could be attributed to the lower specific activity (60 to 129 MBq/mg) of ^{64}Cu-CB-TE1A1P−cetuximab that may have resulted in lower tumor uptake at 48 h postinjection compared to ^{64}Cu-CB-TE1K1P-PEG$_4$-click-cetuximab and ^{64}Cu-DOTA−cetuximab.

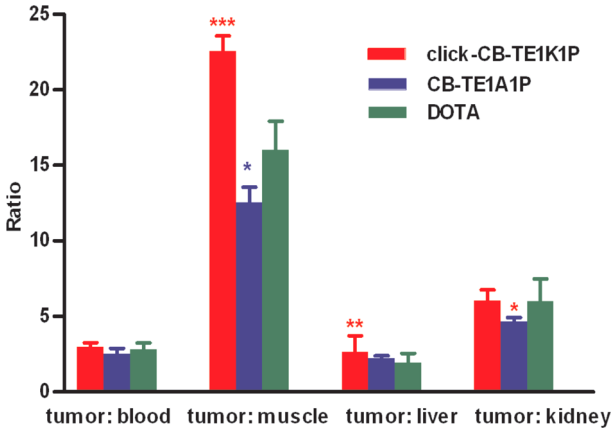

Figure 3. Comparisons of tumor:blood, tumor:muscle, tumor:liver, and tumor:kidney ratios of ^{64}Cu-CB-TE1K1P-PEG$_4$-click-cetuximab, ^{64}Cu-CB-TE1A1P−cetuximab, and ^{64}Cu-DOTA−cetuximab at 48 h postinjection in HCT116 tumor-bearing female nude mice (*$p < 0.05$, **$p < 0.01$, ***$p < 0.001$ vs ^{64}Cu-DOTA−cetuximab[27]).

Small Animal PET/CT Imaging. Small animal PET/CT imaging was performed at 24 and 48 h after injection of ^{64}Cu-CB-TE1A1P−cetuximab and ^{64}Cu-CB-TE1K1P-PEG$_4$-click-cetuximab in HCT116 tumor bearing mice. For both radiotracers, tumor xenografts were clearly visible at 24 and 48 h postinjection. Mice receiving a blocking dose of unlabeled cetuximab showed a significant reduction in uptake of the tracers (Figure 4). The average standardized uptake values (SUV_{avg}) and the tumor-to-muscle ratios were determined for both the blocked and unblocked tumors through region-of-interest (ROI) analysis. The SUVs of the tumor and muscle for ^{64}Cu-CB-TE1A1P−cetuximab were 1.75 and 0.24 respectively, while the tumor and muscle SUVs for ^{64}Cu-CB-TE1K1P-PEG$_4$-click-cetuximab were 1.5 and 0.18. In cohorts injected with a blocking dose, the tumor-to-muscle ratio of ^{64}Cu-CB-TE1A1P−cetuximab was reduced from 7.72 ± 1.59 to 4.44 ± 0.11, and that of ^{64}Cu-CB-TE1K1P-PEG$_4$-click-cetuximab was reduced from 8.07 ± 0.52 to 3.27 ± 0.17 ($p < 0.05$) (Figure 4C), which further confirmed the specificity of the two cross-bridge chelator attached cetuximab conjugates for the EGFR in the HCT116 tumor.

DISCUSSION

The first attempt to conjugate CB-TE1A1P with cetuximab was performed in an aqueous reaction with the assistance of sulfo-NHS. The carboxylate group in CB-TE1A1P was activated by EDC to form an unstable reactive intermediate. Because the hydrolysis of the *o*-acylisourea ester was more prevalent than the coupling reaction with sulfo-NHS, we were not able to produce any conjugated cetuximab by this method. We next tested reactions using DMF as the solvent, with the assistance of NHS and initiated by EDC as the coupling reagent. Activated CB-TE1A1P reacted with NHS to form a semistable amine-reactive ester, which could then form a stable amide bond with the antibody. DMF was evaporated under vacuum before cetuximab aqueous solution was added to the activated CB-TE1A1P. Although conjugation occurred, only an average of 1.5 chelators per cetuximab resulted via this synthetic route, due to the low efficiency of the NHS-aided cross-linking reaction between the CB-TE1A1P and the primary amines of the antibody. Previous studies have shown that the reaction between phosphonic acid groups and amines can occur, but the products quickly hydrolyze and are stable only under strong basic conditions.[28,29] We postulate that the hydrolysis of phosphoramides leads to lower conjugation efficiency between CB-TE1A1P and cetuximab, resulting in low SA of ^{64}Cu-CB-TE1A1P−cetuximab.

Synthesis of radiopharmaceuticals often requires rapid kinetics because of the short half-life. Click chemistry has attractive characteristics, including modularity, reliability, selectivity, rapidity, and efficiency. Cu(I)-catalyzed azide−alkyne cycloaddition (CuAAC) has been widely used for ^{18}F labeled peptides and small molecules and has demonstrated

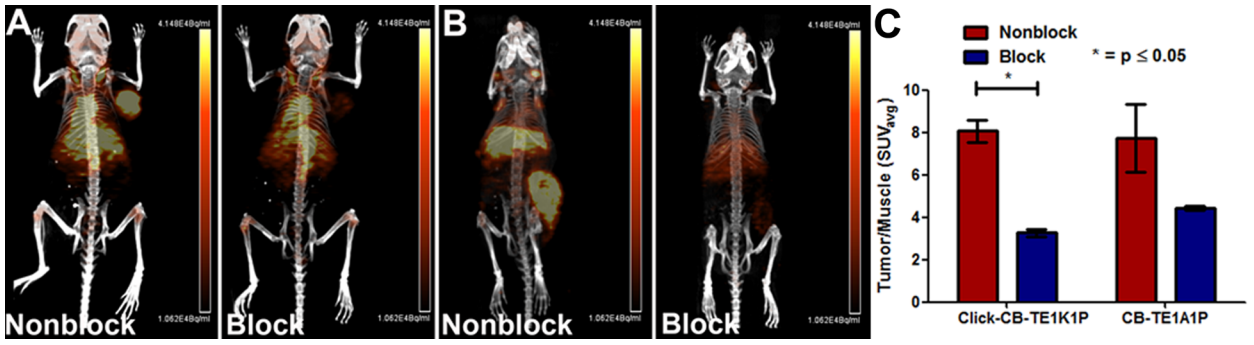

Figure 4. Small animal PET/CT maximum intensity projection images of HCT116 tumor bearing female nude mice at 48 h postinjection of ^{64}Cu-CB-TE1K1P-PEG$_4$-click-cetuximab (A) and ^{64}Cu-CB-TE1A1P−cetuximab (B). One group of mice was pretreated with ∼166−33 equiv of unlabeled cetuximab 24 h prior to probe injection (A and B right panels) while the other group was not pretreated (A and B left panels). Calibration bars are indicative of Bq/mL. (C) Comparison of tumor-to-muscle uptake ratios between blocked and unblocked mice treated with cetuximab probes. Error bars indicative of the standard error of the mean. $N = 2$ for each group.

advantages over conventional conjugation methodologies.[30] However, CuAAC is not ideal for conjugation of chelators because Cu(I) ions may prevent formation of the radiometal−chelate complex. The development of metal-free SPAAC has expanded the use of click chemistry for applications with radiometals.[31−33] To improve the conjugation efficiency, we applied SPAAC to our newly developed chelators. Here we demonstrate the synthesis of cross-bridged chelator−cetuximab conjugates through SPAAC that allows radiolabeling at physiological temperature in high SA. CB-TE1A1P was first modified with commercially available DBCO-amine to form DBCO−CB-TE1A1P in relatively low yield. Then DBCO−CB-TE1A1P was clicked with azide-modified cetuximab. The resulting ^{64}Cu-CB-TE1A1P-click-cetuximab was produced at 40 °C within 60 min in moderate SA (206 to 321 MBq/mg). The binding assay showed comparable binding affinity and B_{max} values of the CB-TE1A1P-click-cetuximab with CB-TE1A1P−cetuximab. However, this conjugate showed different degrees of aggregation from batch to batch. To solve this problem, another cross-bridged macrocyclic chelator, CB-TE1K1P-PEG$_4$-DBCO, with an additional carboxylate pendant arm and a PEG$_4$ linker was designed with the aim of allowing milder labeling conditions and decreased aggregation. The CB-TE1K1P-PEG$_4$-click-cetuximab conjugate was radiolabeled at 37 °C in 30 min in higher SA (548 to 684 MBq/mg). After conjugation of CB-TE1A1P to cetuximab, only one methanephosphonic acid moiety is available for chelating Cu(II). Due to the loss of the carboxylate group and the short linker between the chelator and the antibody, CB-TE1A1P−cetuximab requires 40 °C and relatively longer radiolabeling times (1−2 h),[22,23] which may also account for some of the aggregation problems.

DBCO-PEG$_4$ was attached to the primary amine of CB-TE1K1P and was then conjugated to azide−cetuximab via SPAAC.[22] Via the metal-free click-chemistry route, we were able to avoid hydrolysis of phosphoramides, which resulted in much higher chelator:mAb ratios. The ratio of azide-NHS ester:cetuximab was 20:1, and ∼45% of the NHS esters reacted with primary amines in cetuximab, while the other 55% NHS esters hydrolyzed. The ratio of CB-TE1K1P-PEG$_4$-DBCO:azide−cetuximab was 100:1, driving all azide groups to react with the CB-TE1K1P-PEG$_4$-DBCO, resulting in a chelator:antibody ratio of 9, which increased the SA by 6-fold compared to the SA obtained from the CB-TE1A1P−cetuximab conjugate formed via a NHS-aided reaction.

The *in vivo* performance of ^{64}Cu radiopharmaceuticals is driven in part by the stability of the ^{64}Cu-BFC complex and the SA of the radiotracer. ^{64}Cu-CB-TE1K1P and ^{64}Cu-CB-TE1A1P demonstrated comparable stability to ^{64}Cu-CB-TE2A, both as the metal chelate and after conjugation to peptides.[22,23,34] ^{64}Cu-CB-TE1A1P−cetuximab showed improved biodistribution compared to ^{64}Cu-DOTA−cetuximab, as evident by more rapid blood clearance and the lower uptake in the lung, liver, spleen, and kidney. *In vivo* transchelation of Cu(II) is one factor for nonspecific uptake in normal tissues, and forming stable metal chelates improves biodistribution of peptide conjugates; however, there are no definitive data that this is true for chelator−mAb conjugates. In fact, the tumor:muscle and tumor:kidney ratios of ^{64}Cu-CB-TE1A1P−cetuximab were not significantly better than those of ^{64}Cu-DOTA−cetuximab (p values > 0.05). The low specific activity of ^{64}Cu-CB-TE1A1P−cetuximab may have led to receptor saturation, reducing tumor uptake of the radiotracer. The application of click chemistry enabled increasing SA by enhancing radiolabeling efficiency with a longer linkage between the chelator and mAb and a higher chelator:antibody ratio. ^{64}Cu-CB-TE1K1P−cetuximab demonstrated significantly higher tumor:muscle ($p < 0.001$) and tumor:liver ($p < 0.01$) ratios compared to ^{64}Cu-DOTA−cetuximab.

CONCLUSION

^{64}Cu-CB-TE1A1P−cetuximab was prepared using conventional NHS-aided conjugation, and ^{64}Cu-CB-TE1A1P-click-cetuximab and ^{64}Cu-CB-TE1K1P-PEG$_4$-click-cetuximab were prepared using SPAAC, and the resulting cetuximab conjugates were evaluated as receptor-targeted agents for PET imaging with future applications for radioimmunotherapy (RIT) of tumors overexpressing EGFR. The click chemistry strategy successfully increased the number of chelators that were attached to each antibody and the SA of the corresponding radiopharmaceutical. ^{64}Cu-CB-TE1K1P-PEG$_4$−cetuximab also demonstrated higher tumor:nontumor ratios than ^{64}Cu-CB-TE1A1P−cetuximab. These results provide opportunities for using click chemistry to stably conjugate ^{64}Cu with a wide variety of heat-sensitive biological molecules. ^{64}Cu-CB-TE1K1P-PEG$_4$-click-cetuximab has potential for simultaneously imaging and treating EGFR-positive tumors.

ASSOCIATED CONTENT

Supporting Information

Information on the parameters for the imaging studies. This material is available free of charge via the Internet at http://pubs.acs.org.

AUTHOR INFORMATION

Corresponding Author

*University of Pittsburgh, Department of Radiology, 100 Technology Drive, Suite 452, Pittsburgh, PA 15219. Phone: 412-624-6887. Fax: 412-624-2598. E-mail: andersoncj@upmc.edu.

Author Contributions

‡These two authors have contributed equally to this work

Notes

The authors declare no competing financial interest.

ACKNOWLEDGMENTS

The authors would like to thank Daniel Culy for his work on optimizing conjugation conditions for CB-TE1A1P to cetuximab and Christopher Sherman for technical expertise. This research was funded by NIH/NCI Grants 5R01CA064475 and 5R01CA093375, DOE DE-FG02-08ER64671, and NCI Cancer Center Support Grants P30 CA91842 (WU) and P30 CA047904 (In Vivo Imaging Facility, UPCI).

REFERENCES

(1) Schett, G.; Kiechl, S.; Redlich, K.; Oberhollenzer, F.; Weger, S.; Egger, G.; Mayr, A.; Jocher, J.; Xu, Q.; Pietschmann, P.; Teitelbaum, S.; Smolen, J.; Willeit, J. Soluble RANKL and Risk of Nontraumatic Fracture. *JAMA, J. Am. Med. Assoc.* **2004**, *291*, 1108−1113.

(2) Herbst, R. S.; Shin, D. M. Monoclonal antibodies to target epidermal growth factor receptor-positive tumors: a new paradigm for cancer therapy. *Cancer* **2002**, *94*, 1593−1611.

(3) Brabender, J.; Danenberg, K. D.; Metzger, R.; Schneider, P. M.; Park, J.; Salonga, D.; Holscher, A. H.; Danenberg, P. V. Epidermal growth factor receptor and HER2-neu mRNA expression in non-small

cell lung cancer Is correlated with survival. *Clin. Cancer Res.* **2001**, *7*, 1850−1805.
(4) Serrano, C.; Markman, B.; Tabernero, J. Integration of anti-epidermal growth factor receptor therapies with cytotoxic chemotherapy. *Cancer J.* **2010**, *16*, 226−234.
(5) Cunningham, D.; Humblet, Y.; Siena, S.; Khayat, D.; Bleiberg, H.; Santoro, A.; Bets, D.; Mueser, M.; Harstrick, A.; Verslype, C.; Chau, I.; Van Cutsem, E. Cetuximab monotherapy and cetuximab plus irinotecan in irinotecan-refractory metastatic colorectal cancer. *New Engl. J. Med.* **2004**, *351*, 337−345.
(6) Jonker, D. J.; O'Callaghan, C. J.; Karapetis, C. S.; Zalcberg, J. R.; Tu, D.; Au, H. J.; Berry, S. R.; Krahn, M.; Price, T.; Simes, R. J.; Tebbutt, N. C.; van Hazel, G.; Wierzbicki, R.; Langer, C.; Moore, M. J. Cetuximab for the treatment of colorectal cancer. *New Engl. J. Med.* **2007**, *357*, 2040−2048.
(7) Karapetis, C. S.; Khambata-Ford, S.; Jonker, D. J.; O'Callaghan, C. J.; Tu, D.; Tebbutt, N. C.; Simes, R. J.; Chalchal, H.; Shapiro, J. D.; Robitaille, S.; Price, T. J.; Shepherd, L.; Au, H. J.; Langer, C.; Moore, M. J.; Zalcberg, J. R. K-ras mutations and benefit from cetuximab in advanced colorectal cancer. *New Engl. J. Med.* **2008**, *359*, 1757−1765.
(8) Wen, X.; Wu, Q. P.; Ke, S.; Ellis, L.; Charnsangavej, C.; Delpassand, A. S.; Wallace, S.; Li, C. Conjugation with (111)In-DTPA-poly(ethylene glycol) improves imaging of anti-EGF receptor antibody C225. *J. Nucl. Med.* **2001**, *42*, 1530−1537.
(9) Schechter, N. R.; Wendt, R. E.; Yang, D. J.; Azhdarinia, A.; Erwin, W. D.; Stachowiak, A. M.; Broemeling, L. D.; Kim, E. E.; Cox, J. D.; Podoloff, D. A.; Ang, K. K. Radiation dosimetry of 99mTc-labeled C225 in patients with squamous cell carcinoma of the head and neck. *J. Nucl. Med.* **2004**, *45*, 1683−1687.
(10) Li, W. P.; Meyer, L. A.; Capretto, D. A.; Sherman, C. D.; Anderson, C. J. Receptor-binding, biodistribution, and metabolism studies of 64Cu-DOTA-cetuximab, a PET-imaging agent for epidermal growth-factor receptor-positive tumors. *Cancer Biother. Radiopharm.* **2008**, *23*, 158−171.
(11) Perk, L. R.; Visser, G. W.; Vosjan, M. J.; Stigter-van Walsum, M.; Tijink, B. M.; Leemans, C. R.; van Dongen, G. A. (89)Zr as a PET surrogate radioisotope for scouting biodistribution of the therapeutic radiometals (90)Y and (177)Lu in tumor-bearing nude mice after coupling to the internalizing antibody cetuximab. *J. Nucl. Med.* **2005**, *46*, 1898−1906.
(12) Nayak, T. K.; Regino, C. A.; Wong, K. J.; Milenic, D. E.; Garmestani, K.; Baidoo, K. E.; Szajek, L. P.; Brechbiel, M. W. PET imaging of HER1-expressing xenografts in mice with 86Y-CHX-A″-DTPA-cetuximab. *Eur. J. Nucl. Med. Mol. Imaging* **2010**, *37*, 1368−1376.
(13) Anderson, C. J.; Jones, L. A.; Bass, L. A.; Sherman, E. L.; McCarthy, D. W.; Cutler, P. D.; Lanahan, M. V.; Cristel, M. E.; Lewis, J. S.; Schwarz, S. W. Radiotherapy, toxicity and dosimetry of copper-64-TETA-octreotide in tumor-bearing rats. *J. Nucl. Med.* **1998**, *39*, 1944−1951.
(14) Connett, J. M.; Anderson, C. J.; Guo, L. W.; Schwarz, S. W.; Zinn, K. R.; Rogers, B. E.; Siegel, B. A.; Philpott, G. W.; Welch, M. J. Radioimmunotherapy with a 64Cu-labeled monoclonal antibody: a comparison with 67Cu. *Proc. Natl. Acad. Sci. U.S.A.* **1996**, *93*, 6814−6818.
(15) Connett, J. M.; Buettner, T. L.; Anderson, C. J. Maximum tolerated dose and large tumor radioimmunotherapy studies of 64Cu-labeled monoclonal antibody 1A3 in a colon cancer model. *Clin. Cancer Res.* **1999**, *5*, 3207s−3212s.
(16) Lewis, J. S.; Lewis, M. R.; Cutler, P. D.; Srinivasan, A.; Schmidt, M. A.; Schwartz, S. W.; Morris, M. M.; Miller, J. P.; Anderson, C. J. Radiotherapy and Dosimetry of ^{64}Cu-TETA-Tyr^{3}-Octreotate in a Somatostatin Receptor-positive, Tumor-bearing Rat Model. *Clin. Cancer Res.* **1999**, *5*, 3608−3616.
(17) Eiblmaier, M.; Meyer, L. A.; Watson, M. A.; Fracasso, P. M.; Pike, L. J.; Anderson, C. J. Correlating EGFR expression with receptor-binding properties and internalization of 64Cu-DOTA-cetuximab in 5 cervical cancer cell lines. *J. Nucl. Med.* **2008**, *49*, 1472−1479.
(18) Cai, W.; Chen, K.; He, L.; Cao, Q.; Koong, A.; Chen, X. Quantitative PET of EGFR expression in xenograft-bearing mice using 64Cu-labeled cetuximab, a chimeric anti-EGFR monoclonal antibody. *Eur. J. Nucl. Med. Mol. Imaging* **2007**, *34*, 850−858.
(19) Sprague, J. E.; Peng, Y.; Sun, X.; Weisman, G. R.; Wong, E. H.; Achilefu, S.; Anderson, C. J. Preparation and biological evaluation of copper-64-labeled tyr3-octreotate using a cross-bridged macrocyclic chelator. *Clin. Cancer Res.* **2004**, *10*, 8674−8682.
(20) Wong, E. H.; Weisman, G. R.; Hill, D. C.; Reed, D. P.; Rogers, M. E.; Condon, J. P.; Fagan, M. A.; Calabrese, J. C.; Lam, K.-C.; Guzei, I. A.; Rheingold, A. L. Synthesis and Characterization of Cross-Bridged Cyclams and Pendant-Armed Derivatives and Structural Studies of their Copper(II) Complexes. *J. Am. Chem. Soc.* **2000**, *122*, 10561−10572.
(21) Ferdani, R.; Stigers, D. J.; Fiamengo, A. L.; Wei, L.; Li, B. T.; Golen, J. A.; Rheingold, A. L.; Weisman, G. R.; Wong, E. H.; Anderson, C. J. Synthesis, Cu(II) complexation, 64Cu-labeling and biological evaluation of cross-bridged cyclam chelators with phosphonate pendant arms. *Dalton Trans.* **2012**, *41*, 1938−1950.
(22) Zeng, D.; Ouyang, Q.; Cai, Z.; Xie, X. Q.; Anderson, C. J. New cross-bridged cyclam derivative CB-TE1K1P, an improved bifunctional chelator for copper radionuclides. *Chem. Commun.* **2014**, *50*, 43−45.
(23) Guo, Y. J.; Ferdani, R.; Anderson, C. J. Preparation and Biological Evaluation of Cu-64 Labeled Tyr(3)-Octreotate Using a Phosphonic Acid-Based Cross-Bridged Macrocyclic Chelator. *Bioconjugate Chem.* **2012**, *23*, 1470−1477.
(24) Sun, X.; Rossin, R.; Turner, J. L.; Becker, M. L.; Joralemon, M. J.; Welch, M. J.; Wooley, K. L. An assessment of the effects of shell cross-linked nanoparticle size, core composition, and surface PEGylation on in vivo biodistribution. *Biomacromolecules* **2005**, *6*, 2541−54.
(25) Wang, M.; Caruano, A. L.; Lewis, M. R.; Meyer, L. A.; VanderWaal, R. P.; Anderson, C. J. Subcellular localization of radiolabeled somatostatin analogues: implications for targeted radiotherapy of cancer. *Cancer Res.* **2003**, *63*, 6864−6869.
(26) Eiblmaier, M.; Meyer, L. A.; Anderson, C. J. The role of p53 in the trafficking of copper-64 to tumor cell nuclei. *Cancer Biol. Ther.* **2008**, *7*, 63−69.
(27) Guo, Y.; Parry, J. J.; Laforest, R.; Rogers, B. E.; Anderson, C. J. The role of p53 in combination radioimmunotherapy with 64Cu-DOTA-cetuximab and cisplatin in a mouse model of colorectal cancer. *J. Nucl. Med.* **2013**, *54*, 1621−1629.
(28) Mucha, A.; Grembecka, J.; Cierpicki, T.; Kafarski, P. Hydrolysis of the phosphonamidate bond in phosphono dipeptide analogues - The influence of the nature of the N-terminal functional group. *Eur. J. Org. Chem.* **2003**, *24*, 4797−4803.
(29) Mucha, A.; Kunert, A.; Grembecka, J.; Pawelczak, M.; Kafarski, P. A phosphonamidate containing aromatic N-terminal amino group as inhibitor of leucine aminopeptidase - design, synthesis and stability. *Eur. J. Org. Chem.* **2006**, *41*, 768−772.
(30) Wangler, C.; Schirrmacher, R.; Bartenstein, P.; Wangler, B. Click-chemistry reactions in radiopharmaceutical chemistry: fast & easy introduction of radiolabels into biomolecules for in vivo imaging. *Curr. Med. Chem.* **2010**, *17*, 1092−1116.
(31) Zeng, D.; Zeglis, B. M.; Lewis, J. S.; Anderson, C. J. The growing impact of bioorthogonal click chemistry on the development of radiopharmaceuticals. *J. Nucl. Med.* **2013**, *54*, 829−832.
(32) Zeng, D.; Lee, N. S.; Liu, Y.; Zhou, D.; Dence, C. S.; Wooley, K. L.; Katzenellenbogen, J. A.; Welch, M. J. 64Cu Core-labeled nanoparticles with high specific activity via metal-free click chemistry. *ACS Nano* **2012**, *6*, 5209−5219.
(33) Chen, K.; Wang, X. L.; Lin, W. Y.; Shen, C. K. F.; Yap, L. P.; Hughes, L. D.; Conti, P. S. Strain-Promoted Catalyst-Free Click Chemistry for Rapid Construction of Cu-64-Labeled PET Imaging Probes. *ACS Med. Chem. Lett.* **2012**, *3*, 1019−1023.
(34) Stigers, D. J.; Ferdani, R.; Weisman, G. R.; Wong, E. H.; Anderson, C. J.; Golen, J. A.; Moore, C.; Rheingold, A. L. A new phosphonate pendant-armed cross-bridged tetraamine chelator accel-

erates copper(II) binding for radiopharmaceutical applications. *Dalton Trans.* **2010**, *39*, 1699−1701.